

Stable Limit Set Behavior in a Dynamic Parts Feeder

Kevin M. Lynch Michael Northrop Peng Pan
Laboratory for Intelligent Mechanical Systems
Department of Mechanical Engineering
Northwestern University
Evanston, IL 60208 USA

Abstract

We describe a one-joint planar arm which repeatedly throws and catches parts on its surface, and we demonstrate that proper choice of the throw velocity and arm geometry guarantees that the part will enter a unique recurrent motion pattern from a large set of initial configurations. The resulting system resembles an open-loop stable juggler of polygonal parts.

1 Introduction

The problem of parts feeder design is to design an environment that reduces the uncertainty in the state of a part (or set of parts). The feeder may rely solely on the geometry of specially designed fixtures interacting with a part on a conveyor belt or in a gravity field [3, 8, 2, 12] or specially designed motions of generic surfaces [1], or some combination of geometry, materials, and motion design. In all cases, the goal is to collapse the possible initial states of the part into a smaller set (ideally a singleton).

We describe a simple planar parts feeder consisting of a one joint robot arm that repeatedly throws and catches parts in a gravity field (Figure 1). A “catch” consists of letting the part impact on the stationary arm and come to rest. We show that by the proper choice of the throw velocity and the geometry of the arm, a unique recurrent motion pattern of the part emerges. This behavior emerges without sensing for a large set of initial configurations of the part. Instead of collapsing the possible part configurations to a single point, the device collapses the initial configurations into a cycle similar to a stable limit cycle.

The inspiration for this work comes from the 1JOC parts feeder (Akella *et al* [1]) and work on vibratory parts feeding. In the 1JOC (one joint over conveyor) parts feeder, a one joint revolute robot pushes parts on a constant speed conveyor, and a set of primitives is defined that allows polygonal parts to be moved from any random initial configuration to a desired goal configuration.

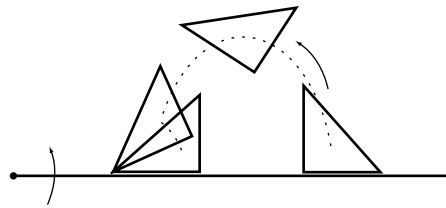


Figure 1: A throw and catch.

In this paper, the conveyor belt is replaced by gravity, and the quasistatic pushing mechanics are replaced by dynamically stable throws and impact mechanics. By analogy to the 1JOC, our system could be called the 1JAG (one joint and gravity). The goal is to create a faster version of the 1JOC. Although we could define planning primitives similar to those for the 1JOC, our purpose in this paper is to study the asymptotic behavior of the system under repeated, identical, low amplitude throws.

The repeated high velocity, low amplitude throws performed by the 1JAG are reminiscent of vibratory motion. One commercially successful vibratory parts feeder is the Sony APOS system. The problem is to design a tray of nests, and a vibratory motion for the tray, so that parts only remain in the nests if they are in the proper orientation. Krishnasamy *et al.* [7] have studied a simplified example of the APOS design problem. Unfortunately, the complex dynamic behavior of a part with non-trivial geometry on a vibrating surface is extremely difficult to analyze, much less design. Our device differs from vibratory feeders in that the arm’s motion is impulsive, and the arm is motionless while the part settles. This assumption makes the system analytically tractable while remaining physically realistic.

Related in spirit to our work is the design of a vertically oscillating table to capture a vertically bouncing ball in a stable periodic orbit (Swanson *et al.* [10]). More generally, the stable discrete-time dynamics of our throwing-catching system brings to mind juggling and hopping sys-

tems [6, 4, 11]. One difference in our work is that the geometry of the part plays an important role in determining the behavior of the system, as is the case for any parts feeder. The key is to show that the mechanics of the throw-catch mapping sends a compact set of the configuration space back to itself—the part cannot escape to infinity. Recurrence follows from this observation. With a weak assumption on an approximated version of the throwing-catching system, it can be shown that all points in the compact set converge to the same forward limit set.

We introduce the notation for the system in Section 2, the mechanics of throwing and catching in Section 3, the existence of stable limit sets in Section 4, and simulations in Section 5.

2 Notation

We define an $x - y$ frame \mathcal{F} at the pivot point of the throwing arm (Figure 2). The gravitational acceleration in \mathcal{F} is $(0, g), g < 0$. The angle of the arm is θ , and a throw begins with the arm horizontal ($\theta = 0$) with the part at rest on the arm. The arm throws the part by rotating counterclockwise to a state $(\theta_r, \dot{\theta}_r)$ and releasing, where $\theta_r, \dot{\theta}_r \geq 0$. The top surface of the arm is a line at $y = h$ when $\theta = 0$. h is called the *offset* and may be positive or negative. The part center of mass is located at (x, y) .

The polygonal part has m edges and m vertices, labeled E^i and $V^i, i = 0 \dots m - 1$, respectively. The boundary vertices of E^i are V^i and V^{i+1} (where V^m is identified with V^0), and i increases as we move counterclockwise around the part. Because the part interacts only with the flat throwing arm, nonconvex parts are treated as their convex hull. The Coulomb friction coefficient between the arm and the part is $\mu > 0$.

When the part rests on E^i under gravity with the arm angle $\theta = 0$, we define a $u^i - v^i$ reference frame \mathcal{F}^i at the center of mass of the part, where the $+v^i$ direction is opposite gravity (see Figure 2). The location of the left vertex of E^i is written (u_l^i, v_l^i) in \mathcal{F}^i , and the right vertex is written (u_r^i, v_r^i) . Note that $v_l^i = v_r^i < 0$. We define the height of the center of mass above the arm surface $d^i = -v_l^i = -v_r^i$. E^i is said to be a *stable edge* if $u_l^i < 0$ and $u_r^i > 0$. The part will stay at rest on a stable edge under small perturbations of the gravitational force or arm angle. The set of stable edges is denoted $\mathcal{S} = \{i | E^i \text{ is stable}\}$.

The mass of the part is m , and its radius of gyration is ρ . The resting state of the part is specified by (i, R) , where i is the edge number ($i \in \mathcal{S}$) and R is the *throwing radius*, or x location of the center of mass when the arm is horizontal. The *part radius* r is the distance from the center of mass to the most distant part vertex, and $d^{\min} = \min_{i \in \mathcal{S}} d^i$ is the distance to the closest point on

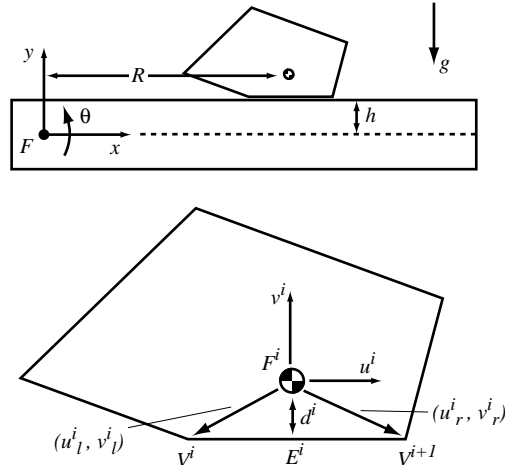


Figure 2: Notation for the throwing and catching arm.

the boundary. We assume that the center of mass is in the interior of the part convex hull, so $d^{\min} > 0$.

3 Throwing and catching

3.1 Throwing

A throw consists of a phase where the manipulator is in contact with the part, called the *carry*, followed by a release and a free flight phase. In this paper all carries satisfy the necessary condition for a *dynamic grasp*.

3.1.1 Dynamic grasp

Definition 3.1. A dynamic grasp occurs when a manipulator in contact with an object accelerates so that there is no relative motion between the object and the manipulator surface (Lynch and Mason [9]).

Example 3.2. A coin resting on an open palm, facing upward, is in a dynamic grasp if the palm is not accelerating downward faster than gravity. A coin in an inverted palm (as when slapping the coin on the back of the other hand after a coin toss) is in a dynamic grasp if the palm accelerates downward faster than gravity.

We assume that throws are accomplished with a dynamic grasp to ensure the repeatability of the release state. It is easy to ensure that a dynamic grasp is robust to variations in the part center of mass location, radius of gyration, or friction coefficient with the thrower. If the part rolls or slips before release, however, differences in these properties will result in different release states.

To test for a dynamic grasp, we assume that the object remains fixed to the manipulator and check if the required

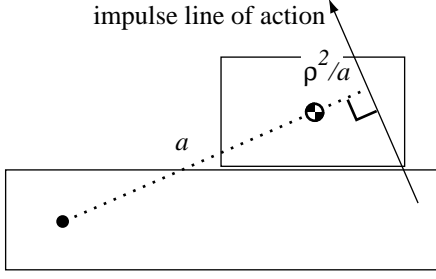


Figure 3: The line of action of the impulse is perpendicular to the line through the thrower pivot and the center of mass, and located a distance ρ^2/a from the center of mass, where $a = \sqrt{R^2 + (h + d^i)^2}$ is the distance between the pivot and the center of mass.

forces of motion can be supplied by the manipulator contact. If so, then a dynamic grasp is a consistent solution to the motion of the object.

We can express the necessary condition for a dynamic grasp in the frame \mathcal{F}^i corresponding to the resting edge E^i . If the arm's angle, angular velocity, and angular acceleration are given by $\theta, \dot{\theta}, \ddot{\theta}$, respectively, then the wrench $\mathbf{w} = (f_{u^i}, f_{v^i}, \tau)^T$ the arm must apply to the part to maintain the dynamic grasp is expressed in \mathcal{F}^i as

$$\mathbf{w} = \ddot{\theta} \begin{bmatrix} -m(h + d^i) \\ mR \\ m\rho^2 \end{bmatrix} + \dot{\theta}^2 \begin{bmatrix} -mR \\ -m(h + d^i) \\ 0 \end{bmatrix} + \begin{bmatrix} -mg \sin \theta \\ -mg \cos \theta \\ 0 \end{bmatrix}.$$

To check if this wrench can be applied by the manipulator contact, we construct the cone of possible contact forces. Assuming Coulomb friction with friction coefficient μ , the cone of contact forces \mathbf{W}^i is all positive linear combinations of the wrenches $\mathbf{w}_1^i, \dots, \mathbf{w}_4^i$ in \mathcal{F}^i , where

$$\begin{aligned} \mathbf{w}_1^i &= (-\mu, 1, u_l^i + \mu v_l^i)^T \\ \mathbf{w}_2^i &= (\mu, 1, u_l^i - \mu v_l^i)^T \\ \mathbf{w}_3^i &= (\mu, 1, u_r^i - \mu v_r^i)^T \\ \mathbf{w}_4^i &= (-\mu, 1, u_r^i + \mu v_r^i)^T. \end{aligned}$$

Note that because \mathbf{W}^i is expressed in the part-fixed frame \mathcal{F}^i , it is independent of the arm configuration. The wrench \mathbf{w} is contained in \mathbf{W}^i if $\mathbf{w}^T(\mathbf{w}_j^i \times \mathbf{w}_k^i) \leq 0$ for the (j, k) pairs $(1, 2), (2, 3), (3, 4), (4, 1)$. These four inequality constraints may be viewed as constraints on the location of the line of force, and they imply that (1) the line of force passes to the right of the left vertex, (2) the line of force is not outside the right edge of the friction cone, (3) the line of force passes to the left of the right vertex, and (4) the line of force is not outside the left edge of the friction cone. These inequality constraints may be solved explicitly as inequality constraints on $\ddot{\theta}$ given the arm state $(\theta, \dot{\theta})$. Any $\ddot{\theta}$ simultaneously satisfying these four constraints will maintain the dynamic grasp.

The part is released at $(\theta_r, \dot{\theta}_r)$. If we set θ_r and the total time of the carry equal to zero, with $\dot{\theta}_r > 0$, the throw becomes impulsive with an impulse \mathbf{p} . For the impulsive throw to be in a dynamic grasp, $\mathbf{p} = (-m(h + d^i)\dot{\theta}_r, mR\dot{\theta}_r, m\rho^2\dot{\theta}_r)^T$ must be contained in \mathbf{W}^i , now considered as an impulse cone. The line of action of \mathbf{p} is independent of $\dot{\theta}_r > 0$, so the test reduces to a simple test on the throwing geometry (Figure 3). We would like to know if the throw is in a dynamic grasp as a function of the throwing radius R .

The four impulse cone constraints can be written

$$R \geq \frac{\rho^2 - v_l^i(h + d^i)}{u_l^i} \quad (1)$$

$$R \geq \frac{-(h + d^i)}{\mu} \quad (2)$$

$$R \geq \frac{\rho^2 - v_r^i(h + d^i)}{u_r^i} \quad (3)$$

$$R \geq \frac{h + d^i}{\mu} \quad (4)$$

Proposition 3.3. *For any stable edge E^i , any offset h , and any friction coefficient $\mu > 0$, there exists a finite radius R_{grasp}^i such that impulsive throws are in a dynamic grasp for all release velocities $\dot{\theta}_r > 0$ and all $R^i \geq R_{grasp}^i$.*

Proof. Since $\mu > 0$ and $u_l^i, u_r^i \neq 0$ by the definition of a stable edge, the lower bounds in the constraints (1)-(4) are finite. The constraints are also independent of $\dot{\theta}_r > 0$. \square

In the rest of the paper, all throws will be assumed to be impulsive throws. We will also assume that the entire part is to the right of the y -axis of \mathcal{F} ; this will eliminate the possibility of the part "stubbing its toe" at the release (left vertex of the resting edge moving downward initially).

3.1.2 Free flight

After an impulsive release at $\theta_r = 0$ and time $t = 0$, the motion of the frame \mathcal{F}^i in \mathcal{F} can be written

$$\begin{bmatrix} x(t) \\ y(t) \\ \phi(t) \end{bmatrix} = \begin{bmatrix} R - (h + d^i)\dot{\theta}_r t \\ h + d^i + R\dot{\theta}_r t + \frac{1}{2}gt^2 \\ \dot{\theta}_r t \end{bmatrix}. \quad (5)$$

The motion of the vertices will also be of interest. If a vertex V is located at (u, v) in \mathcal{F}^i , its motion in \mathcal{F} is

$$\begin{bmatrix} x_V(t) \\ y_V(t) \end{bmatrix} = \begin{bmatrix} x(t) \\ y(t) \end{bmatrix} + \begin{bmatrix} \cos \dot{\theta}_r t & -\sin \dot{\theta}_r t \\ \sin \dot{\theta}_r t & \cos \dot{\theta}_r t \end{bmatrix} \begin{bmatrix} u \\ v \end{bmatrix}. \quad (6)$$

$x_V(t)$ is monotonic decreasing if $\sqrt{u^2 + v^2} < h + d^i$, and it is monotonic increasing if $\sqrt{u^2 + v^2} < -h - d^i$.

3.2 Catching

A catch occurs when the part impacts with the stationary horizontal arm and settles to a stable edge. This can be a very complex process consisting of many impacts. To simplify the analysis, we assume that friction at the impact point is sufficiently high, and the restitution coefficient sufficiently low, that the post-impact velocity of the impact point on the part is zero. This assumption closely approximates actual behavior when the arm is covered with a thin sheet of a highly damping material, such as slow recovery foam. Besides simplifying the analysis of the system, these “sticking” impacts also ensure that the part quickly settles to rest, reducing throw-catch cycle time.

Let $(r_x, r_y)^T$ be the vector from the part center of mass to the impact vertex as measured in \mathcal{F} . The pre-impact velocity of the part at the center of mass is $(\dot{x}^-, \dot{y}^-, \dot{\phi}^-)^T$, and the post-impact velocity is $(\dot{x}^+, \dot{y}^+, \dot{\phi}^+)^T$. The pre- and post-impact velocities satisfy

$$\dot{x}^+ - r_y \dot{\phi}^+ = 0 \quad (7)$$

$$\dot{y}^+ + r_x \dot{\phi}^+ = 0 \quad (8)$$

$$r_x(\dot{y}^+ - \dot{y}^-) - r_y(\dot{x}^+ - \dot{x}^-) = \rho^2(\dot{\phi}^+ - \dot{\phi}^-), \quad (9)$$

where equations (7) and (8) ensure that the post-impact velocity of the impact vertex is zero, and (9) ensures that the impulse passes through the impact point. Equations (7)-(9) can be solved for the post-impact velocity.

After the initial impact, the part rolls without slipping about the impact vertex, with an initial angular velocity of $\dot{\phi}^+$. Rolling continues until another vertex impacts the arm. We solve for the new impact and continue until the part can no longer escape a particular edge. Then the part is considered to have settled to that edge.

For the rest of the paper, we will assume that during rolling the part comes to rest at the first stable edge that comes in contact with the arm. Hence the x motion of the center of mass during rolling is bounded by a constant L . While this assumption is not strictly necessary for the subsequent results, it greatly simplifies the analysis.

An impact is called a *sweet spot catch* if the post-impact velocity is zero ($\dot{\phi}^+ = 0$). The impulse does not change the direction of velocity; it only changes the magnitude (to zero).

3.3 Throwing and catching

For a given h and θ_r , the *throw map* $f : (i_0, R_0) \rightarrow (i_1, R_1)$ maps the initial part configuration (i_0, R_0) to its final configuration (i_1, R_1) after throwing with a dynamic grasp, impacting, and settling. f is only defined for (i_0, R_0) such that E^{i_0} is stable and $R_0 \geq R_{grasp}^{i_0}$. We distinguish between two results of the mapping f :

Jog The part comes to rest on the same edge ($i_0 = i_1$) after a zero net rotation during flight and rolling.

Flip The part comes to rest on a different edge ($i_0 \neq i_1$) (or on the same edge with a net rotation equal to a nonzero integral multiple of 2π).

4 Stable limit sets

In this section we show that by proper choice of h, θ_r , any polygonal part will converge to a unique forward limit set under repeated open-loop impulsive throws. We begin with a definition and a result from dynamical systems theory (e.g., Katok and Hasselblatt [5]).

Definition 4.1. A point $z \in Z$ is nonwandering with respect to a map $b : Z \rightarrow Z$ if for any open set U containing z there is an $N > 0$ such that $b^N(U) \cap U \neq \emptyset$, where b^N indicates N iterations of the map b . The set of all nonwandering points of b is $NW(b)$.

Theorem 4.2. If Z is compact and $b : Z \rightarrow Z$ then $NW(b) \neq \emptyset$.

With Theorem 4.2 as motivation, we search for a compact set of part states Z such that $f : Z \rightarrow Z$.

Proposition 4.3. For any polygonal part, there exists a $\theta_r > 0$ and an h satisfying $0 > h > -d^{\min}$ such that for each stable edge E^i , there exists an R_{flip}^i and R_{max}^i satisfying $R_{grasp}^i < R_{flip}^i < R_{max}^i$, where the following properties hold:

- (i) a throw at $R_{grasp}^i \leq R < R_{flip}^i$ results in a jog with $f(i, R) = (i, R_1)$, $R < R_1 \leq R_{max}^i$, and
- (ii) a throw at $R_{flip}^i \leq R \leq R_{max}^i$ results in a flip with $f(i, R) = (i_1, R_1)$, $R_{grasp}^{i_1} \leq R_1 \leq R_{max}^{i_1}$.

Proof. Plugging the left contact vertex (u_l^i, v_l^i) into Equation (6), differentiating with respect to time, and setting $t = 0$, we find that the initial velocity of the vertex in the x direction after release is $\dot{x}_l(0) = -\theta_r h$. Since $\theta_r > 0$, by choosing $h < 0$, we are guaranteed that the initial motion of the left vertex is in the $+x$ direction. By choosing θ_r sufficiently small, we ensure that a throw at R_{grasp}^i yields a sufficiently small flight time t_f , hence sufficiently small flight rotation angle ϕ_f , that the left vertex is guaranteed to make first contact with the arm at a point further to the right on the arm, and the part will settle again to the same stable edge. The result is a jog with $R_1 > R$.

As R increases from R_{grasp}^i , $\dot{y}(0) = \theta_r R$ increases, yielding a larger amplitude throw, and the above differential analysis is insufficient. During flight, the x velocity of the center of mass is $\dot{x} = -\theta_r(d^i + h)$, where

$h < 0$. If the total rotation angle in flight is ϕ_f and the throw is a jog, then after impact the part rolls about one or more vertices an angle $-\phi_f$ (clockwise) until it comes back to rest on the same edge. Since no local minima of $y(t)$ are encountered during rolling until the part comes to rest on the initial edge (otherwise the part would stop on the corresponding stable edge), we have $(y - h) > d^i$ during rolling. Since $\dot{x} = \dot{\phi}(y - h)$ during rolling and $(y - h) > d^i$ at all times, the total x distance covered by the center of mass to the left during flight is less than the distance to the right during rolling. Therefore, for all jogs, $R_1 > R$.

As R is increased, the larger amplitude of the throw results in a larger ϕ_f and eventually a flip to a new stable edge at $R \geq R_{flip}^i$. For a sufficiently large amplitude throw, the time of flight t_f can be calculated approximately by setting $y(0) = y(t_f)$ in Equation (5). This results in $t_f = -2\theta_r R/g$. Plugging into (5), we get

$$x(t_f) = R\left(1 + \frac{2\theta_r^2(d^i + h)}{g}\right).$$

Since $g < 0$, $x(t_f) < x(0) = R$ if $h > -d^i$. The center of mass moves to the left during flight an amount proportional to R and to θ_r^2 . The center of mass may then roll up to a distance L in either direction. Provided $L < |2\theta_r^2 R(d^i + h)/g|$, which will always be true for sufficiently large R , $R_1 < R$ for the throw and catch.

Therefore, for any h satisfying $0 > h > -d^{min}$ and a sufficiently small θ_r , for each stable edge i the part will jog outward ($R_1 > R$) for sufficiently small $R \geq R_{grasp}^i$. Also, the part center of mass moves to the left during flight an amount proportional to the part radius R . This acts as negative feedback on R , allowing us to place an upper bound R_{max}^i for each stable edge. It remains only to choose θ_r sufficiently small so that a flip never goes to a state (i, R) such that $R < R_{grasp}^i$. \square

Proposition 4.3 leads easily to the following result.

Theorem 4.4. $NW(f) \neq \emptyset$ for an some h, θ_r .

Proof. Let $Z = \bigcup_{i \in \mathcal{S}} (i, [R_{grasp}^i, R_{max}^i])$, as defined in Proposition 4.3. By Proposition 4.3, $f : Z \rightarrow Z$. Z is compact, hence by Theorem 4.2, the nonwandering set in Z is nonempty. \square

This is our first indication of recurrent behavior in open-loop throwing and catching. There is more structure to the throw map f that can be exploited, however. For an appropriate choice of h and θ_r , we define an approximated system characterized by the following behaviors:

- At states $(i, R_{grasp}^i \leq R < R_{flip}^i)$, the part slides outward with continuous motion $R > 0$. The small discrete jogs are replaced with continuous motion.

- The part flips to a new edge when $R \geq R_{flip}^i$.
- The part neither jogs nor flips indefinitely.

This last assumption is based on the fact that as a part jogs outward, the upward release velocity increases linearly with R while the angular velocity is unchanged, hence the part will eventually flip. Since the center of mass moves to the left during flight, flips tend to decrease R , and the part eventually moves back into a jogging range.

This approximation to the actual system is a hybrid system with continuous motion along edges and discrete jumps between edges.

Theorem 4.5. *The approximated hybrid system is guaranteed to enter a unique forward limit set from any state (i, R) such that E^i is stable and $R_{grasp}^i \leq R \leq R_{max}^i$ for some $R_{max}^i \geq R_{flip}^i$.*

Proof. Any state (i, R) , $R_{grasp}^i \leq R < R_{flip}^i$, will eventually reach the same state (i, R_{flip}^i) by jogging. At that point the object will flip, and all future trajectories of the system will be identical. Because the system cycles between jogging and flipping, and because there are only a finite number of stable edges, the system must eventually re-enter a previously visited jog range. At this point, the system will retrace its trajectory; the system has entered its forward limit set. \square

5 Simulations

We have created a simulator based on the mechanics outlined in Section 3, with full rolling simulation. Two test objects, a triangle and a bracket, are shown in Figure 4. In the simulations shown, $g = -220\text{cm/s}^2$, $h = -0.25\text{cm}$ (satisfying Proposition 4.3), and $\theta_r = 80^\circ/s$.

The cycle for the triangle is shown in Figure 5. Note that the cycle has a thickness associated with it, unlike the limit set for the approximate system where discrete jogs are replaced by a velocity. Figure 6 shows that the system is attracted to this cycle from a large range of initial conditions. All edges of the part are in a dynamic grasp for $R \geq 9.32\text{cm}$ and $\mu \geq 0.185$.

Convergence to a cycle for the bracket is shown in Figure 7. All edges (except unstable edge 2) are in a dynamic grasp for $R \geq 13.83\text{cm}$ and $\mu \geq 0.177$.

The cyclic behavior of the parts can be combined with a simple orientation or throwing radius sensor to construct a kind of parts feeder. At some parts of the cycle, the part's orientation is determined uniquely by its position, and at others the part's position is given approximately by its orientation.

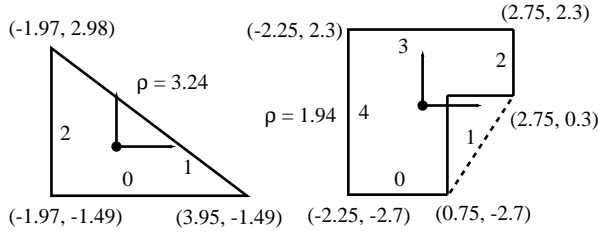


Figure 4: The two objects used in the simulations (distances in cm). Note that edge 2 of the bracket is unstable.

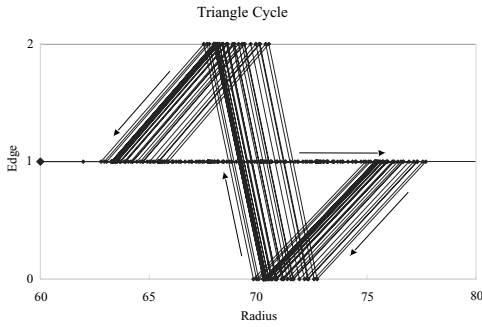


Figure 5: Starting from $(1, 60\text{cm})$, the triangle falls into a repeated motion pattern, consisting of a series of jogs on edge 1, a flip to edge 0, a flip to edge 2, and a flip back to edge 1 where the cycle repeats. The cycle consists of about 8 throws, and 300 throws are shown.

6 Conclusions

By choosing repeated throws and catches, instead of vibrations, as a method for open-loop manipulation of parts, we have shown that strong predictions can be made about the asymptotic behavior of parts with non-trivial geometry (unlike a ball), and that parts can be forced to enter a unique cyclic pattern from a large set of initial configurations. By changing the control parameters θ_r and h , we can modify the cyclic pattern. We are continuing to explore these ideas in the design of dynamic parts feeders.

Acknowledgments

This work was supported by NSF grants IIS-9875469 and IIS-9811571.

References

- [1] S. Akella, W. Huang, K. M. Lynch, and M. T. Mason. Parts feeding on a conveyor with a one joint robot. *Algorithmica*, 26:313–344, 2000.
- [2] R.-P. Berretty, K. Goldberg, L. Cheung, M. Overmars, G. Smith, and F. van der Stappen. Trap design for vibratory bowl feeders. In *IEEE International Conference on Robotics and Automation*, 1999.
- [3] R. C. Brost. Dynamic analysis of planar manipulation tasks. In *IEEE International Conference on Robotics and Automation*, pages 2247–2254, 1992.

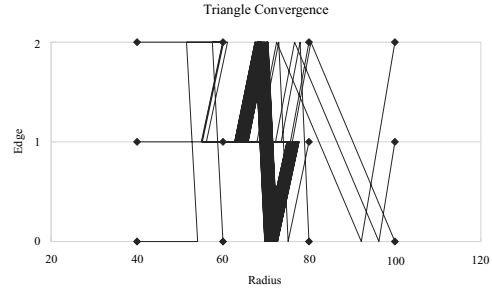


Figure 6: All initial states of the triangle converge to the same cycle. 100 throws are simulated from each diamond.

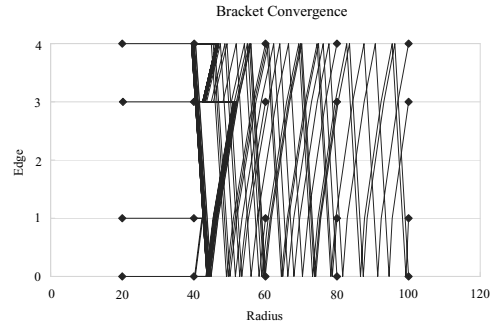


Figure 7: All initial states of the bracket converge to the same cycle consisting of jogs on edge 4, flip to edge 3, jogs on edge 3, flip to edge 1, flip to edge 0, and flip to edge 4, where the cycle repeats. The cycle consists of about 25 throws. 100 throws are simulated from each diamond.

- [4] M. Bühler, D. Koditschek, and P. Kindlmann. Planning and control of a juggling robot. *International Journal of Robotics Research*, 13:101–118, 1994.
- [5] A. Katok and B. Hasselblatt. *Introduction to the Modern Theory of Dynamical Systems*. Cambridge University Press, 1995.
- [6] D. Koditschek and M. Bühler. Analysis of a simplified hopping robot. *International Journal of Robotics Research*, 10:587–605, 1991.
- [7] J. Krishnasamy, M. J. Jakiela, and D. E. Whitney. Mechanics of vibration-assisted entrapment with application to design. *Proc. IEEE International Conference on Robotics and Automation*, pages 838–845, 1996.
- [8] K. M. Lynch. Toppling manipulation. In *IEEE International Conference on Robotics and Automation*, 1999.
- [9] K. M. Lynch and M. T. Mason. Dynamic nonprehensile manipulation: Controllability, planning, and experiments. *International Journal of Robotics Research*, 18(1):64–92, Jan. 1999.
- [10] P. Swanson, R. Burrige, and D. Koditschek. Global asymptotic stability of a passive juggling strategy: A possible parts feeding method. *Mathematical Problems in Engineering*, 3:1983–1988, 1995.
- [11] A. F. Vakakis, J. W. Burdick, and T. K. Caughey. An interesting strange attractor in the dynamics of a hopping robot. *International Journal of Robotics Research*, 10(6):606–618, Dec. 1991.
- [12] T. Zhang, K. Goldberg, R.-P. Berretty, G. Smith, and M. Overmars. The toppling graph: Designing pin sequences for part feeding. In *IEEE International Conference on Robotics and Automation*, 2000.